

RESEARCH PAPER

## From 4'-Hydroxy-2,2':6',2''-Terpyridine Complex of Chromium(III) towards Cr<sub>2</sub>O<sub>3</sub> Nanoparticles: Effects of the Calcination Temperature on the Particle Size and Morphology

Badri Z. Momeni\*, Farzaneh Rahimi

Faculty of Chemistry, K.N. Toosi University of Technology, Tehran, Iran

### ARTICLE INFO

#### Article History:

Received 21 March 2018

Accepted 26 April 2018

Published 01 July 2018

#### Keywords:

Chromium

Cr<sub>2</sub>O<sub>3</sub> Nanoparticles

Fluorescence

Terpyridine

Thermal Analysis

### ABSTRACT

A new chromium (III) complex containing 4'-hydroxy-2,2':6',2''-terpyridine (tpyOH) has been prepared by the reaction of CrCl<sub>3</sub>·6H<sub>2</sub>O with tpyOH in the presence of metallic zinc to afford the new complex [CrCl<sub>3</sub>(tpyOH)] (1). The complex 1 was used as a suitable precursor for the preparation of Cr<sub>2</sub>O<sub>3</sub> nanoparticles by the simple calcination method at three different annealed temperatures of 400, 600, and 800 °C. The structures of the products have been fully characterized by IR, powder X-ray diffraction (XRD), field emission scanning electron microscopy (FESEM) and energy-dispersive X-ray spectroscopy (EDX). The average particle size using Scherrer's equation is calculated to be about 27-36 nm. The results suggest that temperature is an effective way to tailor the morphology and crystallinity of the prepared nanoparticles. The photophysical properties and thermal gravimetric analysis (TGA) of the complex 1 have also been investigated. The emission of 1 exhibits the high-energy intense π→π\* intraligand and low-energy MLCT transitions in DMSO solution. The TGA results show the stability of the complex up to 400 °C after stepwise decomposition of the coordinated ligands.

### How to cite this article

Momeni BZ, Rahimi F. From 4'-Hydroxy-2,2':6',2''-Terpyridine Complex of Chromium(III) towards Cr<sub>2</sub>O<sub>3</sub> Nanoparticles: Effects of the Calcination Temperature on the Particle Size and Morphology. J Nanostruct, 2018; 8(3): 242-250. DOI: 10.22052/JNS.2018.03.003

### INTRODUCTION

Terpyridine ligands act as the suitable ligands for a large variety of transition metal ions since they have three distinct pyridyl groups [1-5]. The terpyridine structural features provide impetus for chemists to design and synthesis of coordination complexes with a wide range of applications from medicine to material science [6-11]. The terpyridine complexes of chromium(III) mainly have been synthesized using anhydrous CrCl<sub>3</sub> in the present of granulated Zn due to the kinetically inert nature of Cr<sup>3+</sup> ion [12-15]. Notably, the lability of Cr(III) ion has been observed in the basic aqueous and methanol solutions of homoleptic and heteroleptic bis-terpyridine complexes of Cr(III) [13].

Preparation of nano-materials is of particular interest because the physical and chemical properties depend on the particle size. Interestingly, the metal coordination compounds have been used as a precursor to prepare the nano metal or metal oxides [16-19]. Thermal decompositions of these compounds led to the preparation of a variety of nanoparticles having different morphologies [20-23]. For example, the structure of the precursor complexes of hydroxyl-terpyridine has influenced on the morphology of the resulting nanoparticles. The mono terpyridine complexes of cobalt resulted in the spherical structures; however, the bis-terpyridine complex of cobalt affords the hexagonal structure [21].

\* Corresponding Author Email: [momeni@kntu.ac.ir](mailto:momeni@kntu.ac.ir)

On the other hand, the average particle size of zinc oxide nanoparticles was increased in the higher calcination temperatures using zinc nitrate as the precursor [22]. Numerous methods have been adopted for the preparation of metal oxide nanoparticles such as hydrothermal, solvothermal, precipitation and sol-gel methods [21, 24-27]. Nano metal oxides exhibit drastically different properties compared to the corresponding bulk ones due to their different sizes and shapes which has been resulted in the distinctive quantum features [28]. Cr<sub>2</sub>O<sub>3</sub> (chromium sesquioxide) is an important technological material which has been attracted increasing interest in recent years due to its properties and applications such as catalysis [29], humidity sensing [30] and advanced colorant [31].

Herein, we report the preparation and characterization of the new complex [Cr(tpyOH)Cl<sub>3</sub>].2H<sub>2</sub>O (**1**). The Cr<sub>2</sub>O<sub>3</sub> NPs have been prepared using complex **1** as the new precursor. The heat treatment of **1** in three different temperatures were done to study the effect of the calcining temperature on particles size and morphology. The results show that the morphology and size of resulting Cr<sub>2</sub>O<sub>3</sub> NPs is dependent upon the thermolysis temperature. In addition, the thermal and luminescence behaviors of the complex **1** were investigated.

## MATERIALS AND METHODS

### General Remarks

Elemental analysis was performed by Thermo Finnigan Flash Ea 1112 elemental analyzer. IR spectra in the 4000-400 cm<sup>-1</sup> were recorded on KBr pellets using ABB Bomem Model FTLA200-100 spectrophotometer. The electronic absorption spectra were recorded on a PerkinElmer Lambda 25 UV-Vis spectrophotometer, using a 1 cm path length cell. The luminescence property was performed using a Perkin-Elmer LS55 luminescence spectrometer. Experiments were carried out at room temperature. The excitation and emission band pass (slit) was 10 nm with the scan rate of 1000 nm/min. The electric conductivity (EC) of complex was measured by a 4520 bench conductivity meter using a conductivity cell for manual sampling which was purchased from Azar Electrode (Urmia, Iran). TGA-DTA data was collected by SHIMADZU TGA-50 at a heating rate of 10 K min<sup>-1</sup> under N<sub>2</sub> atmosphere. The XRD patterns were recorded in the 2θ range of 10-80° using a PHILIPS PW1730 by CuKα radiation,

$k\alpha = 1.5406\text{Å}$ . Field emission scanning electron microscopy (FESEM) images were obtained using a TESCAN MIRA II (Scanning Electron Microscope) device, operating at an accelerating voltage 10 kV, equipped with energy dispersive spectroscopy (EDX). 4'-Hydroxy-2,2':6',2''-terpyridine (tpyOH) was prepared according to the literature [32].

### Synthesis of [Cr(tpyOH)Cl<sub>3</sub>].2H<sub>2</sub>O (**1**)

CrCl<sub>3</sub>.6H<sub>2</sub>O (27 mg, 0.10 mmol) and tpyOH (25 mg, 0.10 mmol) were suspended in MeOH (10 mL). The reaction mixture was heated to reflux and then granulated zinc (19 mg, 0.26 mmol) was added. After a few minutes, the mixture turned dark brown and a green precipitate formed. The reaction mixture was then heated at reflux for 6 h, after which it was filtered, leaving excess zinc in the reaction flask. Then the green precipitate of **1** was collected by centrifugation and washed with methanol. Yield: 65 %; m.p. 254-256 °C (dec.). Anal. Calc. for C<sub>15</sub>H<sub>11</sub>Cl<sub>3</sub>CrN<sub>3</sub>O.2H<sub>2</sub>O: C, 40.61; H, 3.41; N, 9.47. Found: C, 41.00; H, 3.28; N, 7.03. Selected IR data (KBr, cm<sup>-1</sup>): 3543 (O-H), 2720 (=C-H), 1627 (C=N, C=O), 1261 (C-O), 1156, 862, 792, 612. UV-vis (DMSO): λ<sub>max</sub>/nm (ε/M<sup>-1</sup> cm<sup>-1</sup>); 276, 310, 324. TGA: calc. by formula C<sub>15</sub>H<sub>11</sub>Cl<sub>3</sub>CrN<sub>3</sub>O.3H<sub>2</sub>O: 3H<sub>2</sub>O % = 11.71, 1Cl % = 7.68, 2Cl % = 15.36, tpyOH % = 54.00. Determined: 3H<sub>2</sub>O % = 10.53, 1 Cl % = 9.63, 2 Cl % = 13.03, tpyOH % = 54.09.

### Preparation of Cr<sub>2</sub>O<sub>3</sub> nanoparticles

The complex **1** was subjected to heat treatment at 400, 600, and 800°C in air, respectively. After 2h, they were allowed to cool to room temperature to form green Cr<sub>2</sub>O<sub>3</sub> nanoparticles.

## RESULTS AND DISCUSSION

The reaction of CrCl<sub>3</sub>.6H<sub>2</sub>O with tpyOH in methanol affords the green complex of [Cr(tpyOH)Cl<sub>3</sub>] (**1**) as shown in Fig. 1. The product has been characterized by elemental analysis, IR, UV-visible and fluorescence spectroscopy.

The results of elemental analysis of the complex are in good agreement with the proposed formula. However, there are two probable structures for the complex **1**, according to the elemental analysis; [Cr(tpyOH)Cl<sub>3</sub>] or ionic complex [Cr(tpyOH)Cl<sub>2</sub>]<sup>+</sup>Cl<sup>-</sup>. The results of the electric conductivity of a DMSO solution of complex **1** were below 0.4 μs which suggests the presence of the neutral structure for the complex [Cr(tpyOH)Cl<sub>3</sub>] (**1**).

It has been shown that the terpyridine metal

complexes exhibit d-d transitions in DMF solution in the visible region and intra-ligand transitions in the UV region [14]. The d<sup>3</sup> chromium(III) ion in a perfect octahedral geometry is expected to have three absorption bands due to the electron transitions from <sup>4</sup>A<sub>2g</sub> as the electronic ground state to the <sup>4</sup>T<sub>2g</sub>, <sup>4</sup>T<sub>1g</sub>(F), and <sup>4</sup>T<sub>1g</sub>(P) as the excited states. Usually, the d-d bands originating from <sup>4</sup>A<sub>2g</sub> → <sup>4</sup>T<sub>2g</sub>, <sup>4</sup>A<sub>2g</sub> → <sup>4</sup>T<sub>1g</sub>(F) fall in the visible region

and <sup>4</sup>A<sub>2g</sub> → <sup>4</sup>T<sub>1g</sub>(P) in the UV region [14]. The complex has a pseudo octahedral geometry with a lower symmetry than normal octahedral. Therefore, the splitting of the orbitally degenerate terms could be possible. Accordingly, the lower symmetry of the complex led to the observation of three bands in the UV-Vis spectrum at 277, 310, and 325 nm, respectively, as shown in Fig. 2. The lowest energy band is originating from the <sup>4</sup>A<sub>2g</sub> → <sup>4</sup>T<sub>2g</sub> (from Oh

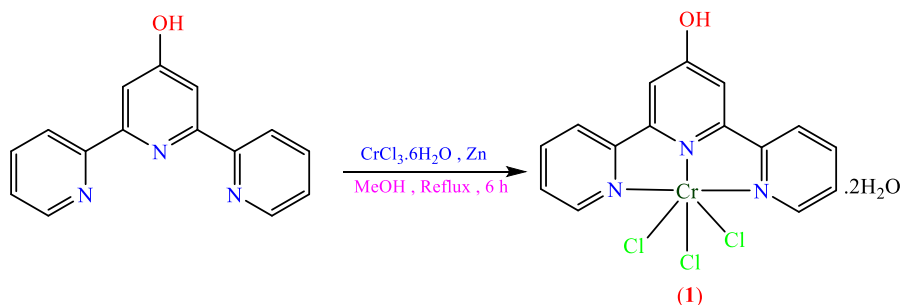


Fig. 1. Preparation of [Cr(tpyOH)Cl<sub>3</sub>]. 2H<sub>2</sub>O (1).

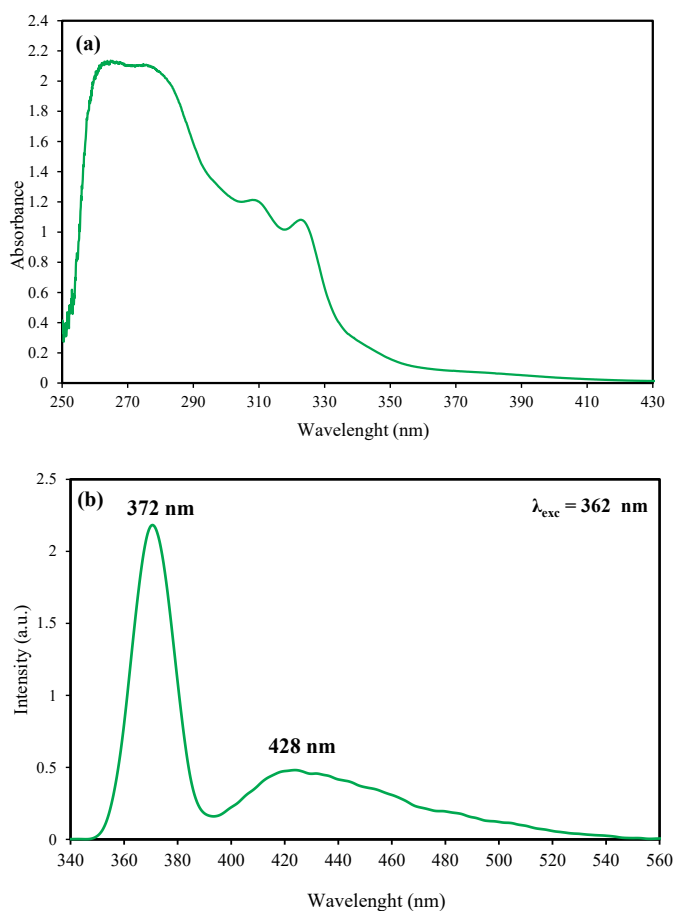


Fig. 2. (a) UV-Vis and (b) emission spectrum of a DMSO solution of complex 1 upon the excitation at  $\lambda_{ex} = 362$  nm at room temperature.

symmetry) transition, which directly corresponds to 10Dq [33].

The fluorescence spectra of complex **1** and the free ligand of tpyOH have been investigated at room temperature in DMSO solution with a concentration of  $1 \times 10^{-5}$  M. The complex exhibits a strong emission at 372 nm upon the excitation at  $\lambda_{\text{exc}} = 362$  nm as well a broad emission band at 428 nm, as illustrated in Fig. 2. The emission at 372 nm is due to the ligand based intramolecular emission  $\pi \rightarrow \pi^*$  (IL). Such a similar band was observed at 358 nm for a DMSO solution of the free tpyOH ligand upon excitation at  $\lambda_{\text{exc}} = 330$  nm. On the other hand, there is a broad emission band at 428 nm could be assigned to the metal to ligand charge transfer (MLCT) [14, 34]. Such a bathochromic shift has been observed in the formation of hydroxyterpyridine complex of cobalt relative to the free tpyOH ligand [35]. The outstanding luminescence properties of terpyridine ligands along with their ability to coordinate to a large number of metal ions have driven these kind of ligands to be use as a suitable receptors for design of metal chemosensors [10].

The thermal property of the complex **1** was studied and the results are shown in Fig. 3. There are four major steps in TGA curve of the complex **1** as shown in Fig. 3. The first weight loss occurs at 51-97 °C and it could be corresponded to evaporation of three adsorbed water molecules with calculated amount of 11.71 % in contrast with the experimental amount of 10.53 % for this step. The second step with 9.63 % weight loss is in the temperature range of 122-147 °C and it could be referred to the loss of the first chloride moiety with calculated amount of 7.68 %. Further decomposition of the complex at 254-286 °C

(13.03 %) could be due to the loss of the other two coordinated chlorides with calculated amount of 15.36 %. The final step at 454-467 °C is the largest weight loss in the curve (54.09 %) and it could be corresponded to loss of tpyOH moiety (calc. 54.00 %). The TGA curve indicates that the weight loss of terpyridine is observed in higher temperatures relative to the other steps which could be raised due to the higher bond dissociation energies of the chromium-nitrogen bonds. The IR spectrum of the complex shows an absorbance band at 1627  $\text{cm}^{-1}$  which could be assigned to the presence of tpyOH as well as the  $\nu = (\text{O-H})$  at 3543  $\text{cm}^{-1}$  (Fig. 4) [14].

#### Formation and characterization of metal oxide nanoparticles

The thermal decomposition of the complex **1** led to preparation of Cr<sub>2</sub>O<sub>3</sub> nanoparticles. In order to find the effect of the calcination temperature on the nanoparticle sizes and morphologies, the calcination process was carried out in three different temperatures of 400, 600, and 800 °C, respectively.

The FTIR spectra of Cr<sub>2</sub>O<sub>3</sub> nanoparticles are shown in Fig. 4. The broad bands at 3434 and 3440  $\text{cm}^{-1}$  are assigned to both  $\nu_{\text{s}(\text{H-O-H})}$  and  $\nu_{\text{a}(\text{H-O-H})}$  of adsorbed water molecules in the structure of prepared nanoparticles at 400 and 600 °C, respectively. Metal oxide Cr<sub>2</sub>O<sub>3</sub> generally reveal absorption bands below 1000  $\text{cm}^{-1}$  due to the inter-atomic vibrations. Two sharp bands in the region of 500 and 600  $\text{cm}^{-1}$  attributed to the Cr-O stretching modes. This results further approved the formation of Cr<sub>2</sub>O<sub>3</sub> nanoparticles by simple thermal decomposition of complex **1** [36].

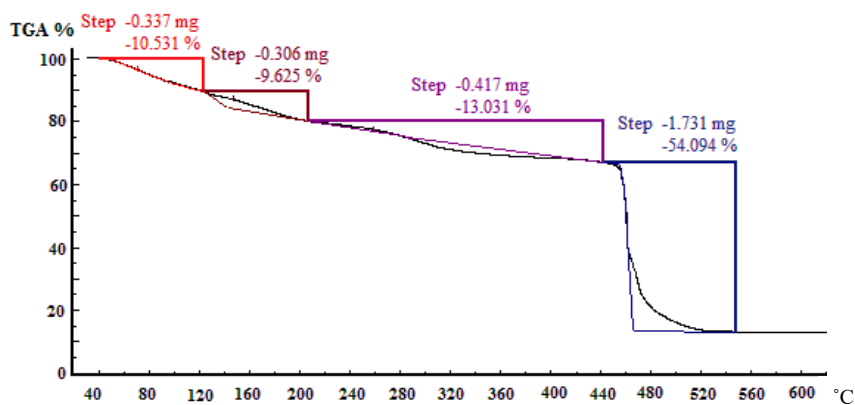


Fig. 3. Thermal analysis of [Cr(tpyOH)Cl<sub>3</sub>] (**1**).

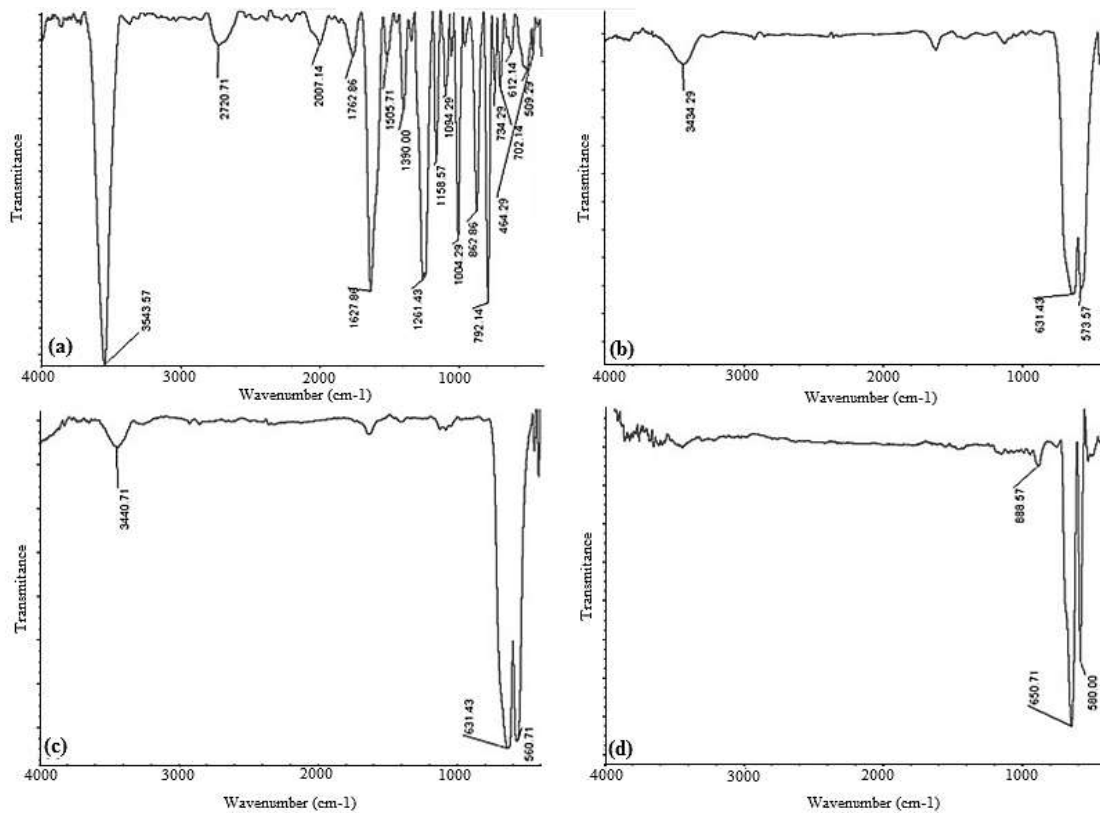


Fig. 4. The IR spectra of (a) [Cr(tpyOH)Cl<sub>3</sub>] (1) and prepared Cr<sub>2</sub>O<sub>3</sub> nanoparticles at (b) 400 °C, (c) 600 °C and (d) 800 °C.

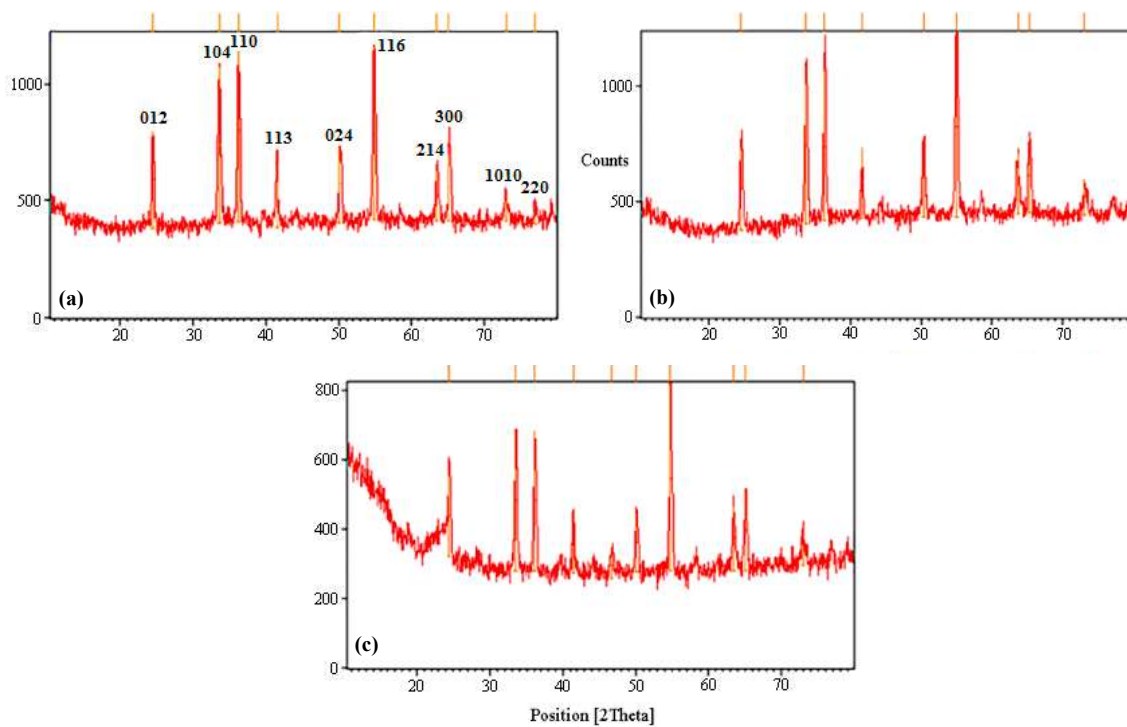


Fig. 5. The XRD patterns of prepared Cr<sub>2</sub>O<sub>3</sub> nanoparticles at (a) 400, (b) 600 and (c) 800 °C.

The XRD patterns of the as-synthesized powders at 400, 600, and 800 °C have been shown in Fig. 5. The diffractograms indicate the presence of prominent peaks corresponding to (0 1 2), (1 0 4), (1 1 0), (1 1 3), (0 2 4), (1 1 6), (2 1 4), (3 0 0), (1 0 10) and (2 2 0) plans the mineral Cr<sub>2</sub>O<sub>3</sub> (eskolaite). Therefore, it confirms the synthesis of pure and crystalline Cr<sub>2</sub>O<sub>3</sub> in accordance with Ref-code 98-004-5808. The crystallite sizes were calculated from the diffraction peaks due to the Scherrer formula as shown in eq. (1) [37].

$$d = \frac{\kappa\lambda}{\beta \cos \theta} \quad (1)$$

Where  $\kappa$  is a constant (ca. 0.9);  $\lambda$  is the X-ray

wavelength used in XRD (1.5418 Å);  $\theta$  the Bragg angle and  $\beta$  is the pure diffraction broadening of a peak at half-height. The peak broadening suggests very small crystallites. In fact, applying Scherrer's relation to the XRD peaks indicates that the average crystallite sizes are 34, 27, and 36 nm for the as-prepared nanoparticles at 400, 600 and 800 °C, respectively.

The morphology of the resulting powders was investigated by FESEM as shown in Fig. 6. The FESEM image of Cr<sub>2</sub>O<sub>3</sub> nanoparticles treated at 400 °C reveals the spherical shapes particles with apparently agglomerates (Fig. 6a). By enhancing the calcination temperature to 600 °C, the morphology of nanoparticles changes to

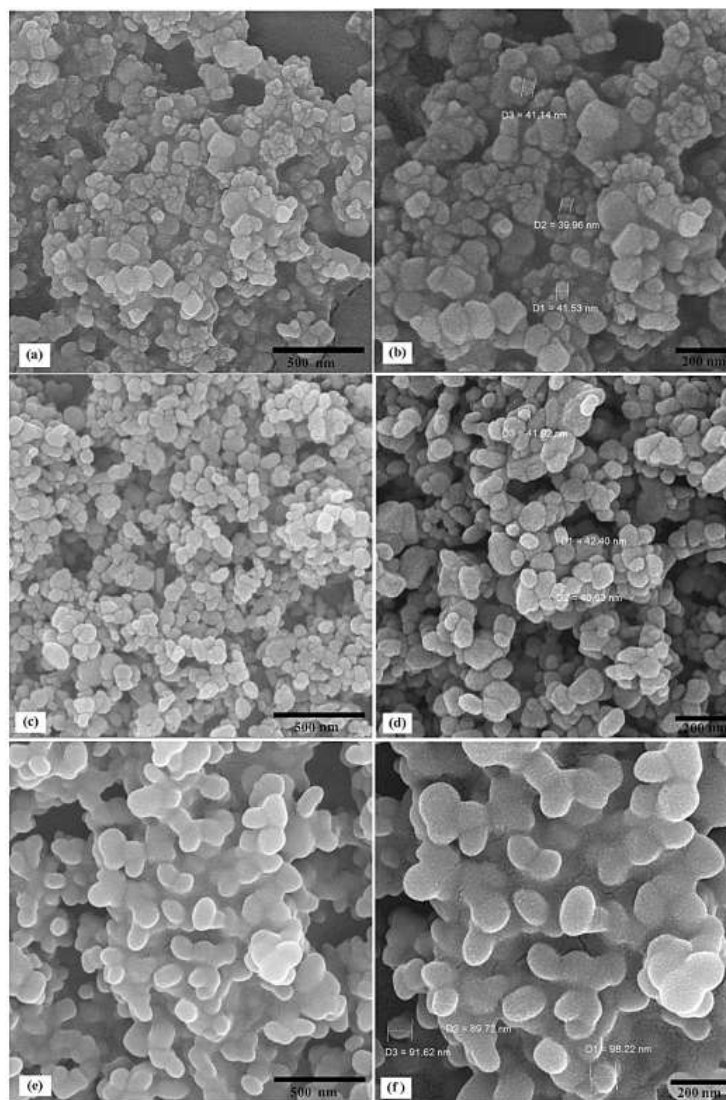


Fig. 6. The FESEM images of prepared Cr<sub>2</sub>O<sub>3</sub> nanoparticles at (a, b) 400, (c, d) 600, and (e, f) 800 °C.

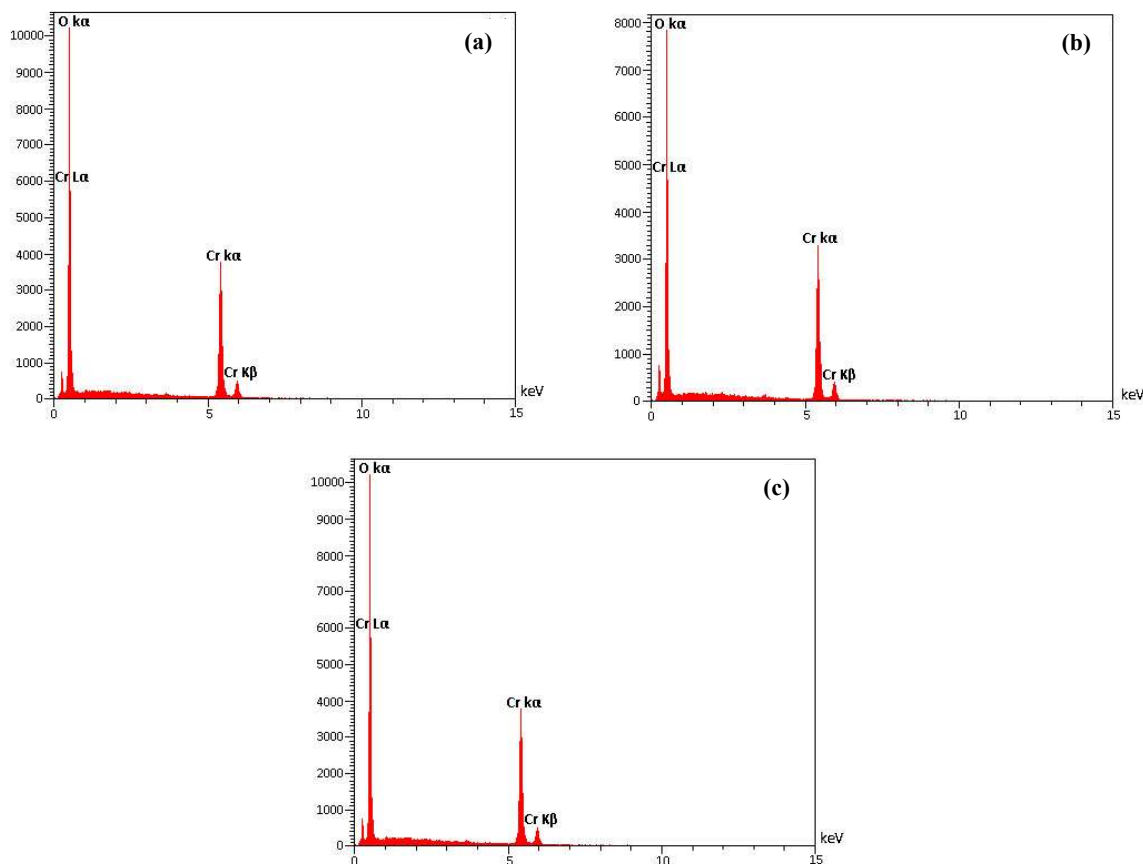


Fig. 7. The EDX pattern of prepared Cr<sub>2</sub>O<sub>3</sub> nanoparticles at (a) 400, (b) 600 and (c) 800 °C.

uniform spherical shapes (Fig. 6b). The calcination temperature of 800 °C reveals that the as-prepared nanoparticles have the same morphology as the prepared nanoparticles at 600 °C. However, it can be seen that the particles possess a spherical shaped morphology with the small agglomeration. To investigate the atomic percentage of the nanoparticles, the chemical composition is checked by energy dispersive X-ray diffractograms which are shown in Fig. 7a-7c, respectively. The results show the presence of elemental Cr and O and it confirms the successful synthesis of Cr<sub>2</sub>O<sub>3</sub> nanoparticles.

## CONCLUSION

In conclusion, a new complex of 4'-hydroxy-2,2'-6',2''-terpyridine of chromium(III) was synthesized and used as a new precursor for the preparation of Cr<sub>2</sub>O<sub>3</sub> nanoparticles. The photophysical properties of the complex in DMSO solution at room temperature shows two emissions resulting from the  $\pi$ - $\pi^*$  intraligand

and MLCT interactions. The IR spectra of all nanoparticles show the absorption bands of Cr-O stretching modes as well as the O-H stretching modes about 3400 cm<sup>-1</sup> for the resulting nanoparticles at 400 and 600 °C. The XRD pattern of the nanoparticles revealed the pure and crystalline Cr<sub>2</sub>O<sub>3</sub> (eskolaite). However, the finest nanoparticles were obtained at 600 °C calculated Scherrer's relation (27 nm). The nanoparticles increased in size in the calcination temperatures of 400 and 800 °C. The morphology of nanoparticles is also dependent on the calcination temperature. Thus, the agglomeration was observed at 400 °C and by increasing the temperature to 600 °C, the morphology of nanoparticles changed to uniform spherical shapes. Accordingly, the EDX results show the presence of elemental Cr and O which confirms the successful synthesis of Cr<sub>2</sub>O<sub>3</sub> nanoparticles. Moreover, the results show that the Cr<sub>2</sub>O<sub>3</sub> nanoparticles with smaller size and better morphology can be obtained at calcination temperature of 600 °C.

## ACKNOWLEDGMENT

We would like to thank the Science Research Council of K.N. Toosi University of Technology for financial support.

## CONFLICT OF INTEREST

The authors declare that there are no conflicts of interest regarding the publication of this manuscript.

## REFERENCES

- Hofmeier H, Schubert US. Recent developments in the supramolecular chemistry of terpyridine–metal complexes. *Chem Soc Rev*. 2004;33(6):373-99.
- Martinez-Vargas S, Valdés-Martínez J, Martínez AI. Supramolecular architectures of Cu(II) with terpyridine and pyridyl-carboxylates. *Journal of Molecular Structure*. 2011;1006(1-3):425-33.
- Liu R, Li Z, Zhu H, Sun W. Synthesis and photophysical studies of back-to-back dinuclear platinum terpyridine complexes with different substituents on the bridging ligand. *Inorganica Chimica Acta*. 2012;387:383-9.
- Ma Z, Lu W, Liang B, Pombeiro AJL. Synthesis, characterization, photoluminescent and thermal properties of zinc(II) 4'-phenyl-terpyridine compounds. *New Journal of Chemistry*. 2013;37(5):1529.
- Aroua S, Todorova TK, Hommes P, Chamoreau L-M, Reissig H-U, Mougél V, et al. Synthesis, Characterization, and DFT Analysis of Bis-Terpyridyl-Based Molecular Cobalt Complexes. *Inorganic Chemistry*. 2017;56(10):5930-40.
- Manikandamathavan VM, Rajapandian V, Freddy AJ, Weyhermüller T, Subramanian V, Nair BU. Effect of coordinated ligands on antiproliferative activity and DNA cleavage property of three mononuclear Cu(II)-terpyridine complexes. *European Journal of Medicinal Chemistry*. 2012;57:449-58.
- Çeşme M, Gölcü A, Demirtaş I. New metal based drugs: Spectral, electrochemical, DNA-binding, surface morphology and anticancer activity properties. *Spectrochimica Acta Part A: Molecular and Biomolecular Spectroscopy*. 2015;135:887-906.
- Bolink HJ, Cappelli L, Coronado E, Gaviña P. Observation of Electroluminescence at Room Temperature from a Ruthenium(II) Bis-Terpyridine Complex and Its Use for Preparing Light-Emitting Electrochemical Cells. *Inorganic Chemistry*. 2005;44(17):5966-8.
- Yao KPC, Frith JT, Sayed SY, Bardé F, Owen JR, Shao-Horn Y, et al. Utilization of Cobalt Bis(terpyridine) Metal Complex as Soluble Redox Mediator in Li–O<sub>2</sub> Batteries. *The Journal of Physical Chemistry C*. 2016;120(30):16290-7.
- Wu W-J, Wang J, Chen M, Qian D-J, Liu M. Terpyridine-Functionalized NanoSiO<sub>2</sub> Multi-Dentate Linkers: Preparation, Characterization and Luminescent Properties of Their Metal–Organic Hybrid Materials. *The Journal of Physical Chemistry C*. 2017;121(4):2234-42.
- Abd-El-Aziz AS, Piffold JL, Momeni BZ, Proud AJ, Pearson JK. Design of coordination polymers with 4'-substituted functionalized terpyridyls in the backbone and pendent cyclopentadienyliron moieties. *Polym Chem*. 2014;5(10):3453-65.
- Cloete N, Visser HG, Roodt A. mer-Trichloro(2,2',2''-terpyridine)chromium(III) dimethyl sulfoxide solvate. *Acta Crystallographica Section E Structure Reports Online*. 2006;63(1):m45-m7.
- Cloete N, Visser HG. (Acetylacetonato) aqua(2,2',2''-terpyridine)chromium(III) bis(perchlorate) dihydrate hexamethylphosphoramide solvate. *Acta Crystallographica Section E Structure Reports Online*. 2007;63(12):m3069-m70.
- Constable EC, Housecroft CE, Neuburger M, Schönle J, Zampese JA. The surprising lability of bis(2,2':6',2''-terpyridine)chromium(III) complexes. *Dalton Trans*. 2014;43(19):7227-35.
- Schönle J, Constable EC, Housecroft CE, Neuburger M. Tuning peripheral  $\pi$ -stacking motifs in {Cr(tpy)<sub>2</sub>}<sup>3+</sup> domains (tpy=2,2':6',2''-terpyridine). *Inorganic Chemistry Communications*. 2015;53:80-3.
- Salavati-Niasari M, Davar F, Mir N. Synthesis and characterization of metallic copper nanoparticles via thermal decomposition. *Polyhedron*. 2008;27(17):3514-8.
- Sadeghzadeh H, Morsali A, Yilmaz VT, Büyükgüngör O. Synthesis of PbO nano-particles from a new one-dimensional lead(II) coordination polymer precursor. *Materials Letters*. 2010;64(7):810-3.
- Khalaji AD, Nikookar M, Fejfarova K, Dusek M. Synthesis of new cobalt(III) Schiff base complex: A new precursor for preparation Co<sub>3</sub>O<sub>4</sub> nanoparticles via solid-state thermal decomposition. *Journal of Molecular Structure*. 2014;1071:6-10.
- Salavati-Niasari M, Khansari A. Synthesis and characterization of Co<sub>3</sub>O<sub>4</sub> nanoparticles by a simple method. *Comptes Rendus Chimie*. 2014;17(4):352-8.
- Masoomi MY, Morsali A. Applications of metal–organic coordination polymers as precursors for preparation of nano-materials. *Coordination Chemistry Reviews*. 2012;256(23-24):2921-43.
- Momeni BZ, Rahimi F, Rominger F. Preparation of Co<sub>3</sub>O<sub>4</sub> Nanoparticles via Thermal Decomposition of Three New Supramolecular Structures of Co(II) and (III) Containing 4'-Hydroxy-2,2':6',2''-Terpyridine: Crystal Structures and Thermal Analysis Studies. *Journal of Inorganic and Organometallic Polymers and Materials*. 2017;28(1):235-50.
- Al-Hada NM, Saion E, Shaari AH, Kamarudin MA, Gene SA. The Influence of Calcination Temperature on the Formation of Zinc Oxide Nanoparticles by Thermal-Treatment. *Applied Mechanics and Materials*. 2013;446-447:181-4.
- Goudarzi M, Bazarganipour M, Salavati-Niasari M. Synthesis, characterization and degradation of organic dye over Co<sub>3</sub>O<sub>4</sub> nanoparticles prepared from new binuclear complex precursors. *RSC Adv*. 2014;4(87):46517-20.
- Kumaresan N, Ramamurthi K, Ramesh Babu R, Sethuraman K, Moorthy Babu S. Hydrothermally grown ZnO nanoparticles for effective photocatalytic activity. *Applied Surface Science*. 2017;418:138-46.
- Sun T-W, Zhu Y-J, Qi C, Ding G-J, Chen F, Wu J.  $\alpha$ -Fe<sub>2</sub>O<sub>3</sub> nanosheet-assembled hierarchical hollow mesoporous microspheres: Microwave-assisted solvothermal synthesis and application in photocatalysis. *Journal of Colloid and Interface Science*. 2016;463:107-17.
- Gopinath S, Philip J. Preparation of metal oxide nanoparticles of different sizes and morphologies, their characterization

- using small angle X-ray scattering and study of thermal properties. *Materials Chemistry and Physics*. 2014;145(1-2):213-21.
27. Sui R, Charpentier P. Synthesis of Metal Oxide Nanostructures by Direct Sol–Gel Chemistry in Supercritical Fluids. *Chemical Reviews*. 2012;112(6):3057-82.
  28. Gawande MB, Goswami A, Felpin F-X, Asefa T, Huang X, Silva R, et al. Cu and Cu-Based Nanoparticles: Synthesis and Applications in Catalysis. *Chemical Reviews*. 2016;116(6):3722-811.
  29. Singh KK, Senapati KK, Borgohain C, Sarma KC. Newly developed Fe<sub>3</sub>O<sub>4</sub>–Cr<sub>2</sub>O<sub>3</sub> magnetic nanocomposite for photocatalytic decomposition of 4-chlorophenol in water. *Journal of Environmental Sciences*. 2017;52:333-40.
  30. Jayamurugan P, Mariappan R, Premnazeer K, Ashokan S, Subba Rao YV, Seshagiri Rao NVSS, et al. Investigation of Annealing Temperature on Structural and Morphological Properties of Cr<sub>2</sub>O<sub>3</sub> Nanoparticles for Humidity Sensor Application. *Sensing and Imaging*. 2017;18(1).
  31. Li P, Xu H, Zhang Y, Li Z, Zheng S, Bai Y. The effects of Al and Ba on the colour performance of chromic oxide green pigment. *Dyes and Pigments*. 2009;80(3):287-91.
  32. Constable EC, Ward MD. Synthesis and coordination behaviour of 6',6"-bis(2-pyridyl)-2,2' : 4,4" : 2",2"-quaterpyridine; 'back-to-back' 2,2' : 6',2"-terpyridine. *J Chem Soc, Dalton Trans*. 1990(4):1405-9.
  33. Lever ABP. *Inorganic Electronic Spectroscopy*, The Netherlands, Amsterdam, Elsevier, 2<sup>nd</sup> Ed. 1986.
  34. Padhi SK, Saha D, Sahu R, Subramanian J, Manivannan V. Synthesis, structure, optical and magnetic properties of [CrL(X)<sub>3</sub>], {L=4'-(2-pyridyl)-2,2':6',2"-terpyridine; X=Cl<sup>-</sup>, N<sub>3</sub><sup>-</sup>, NCS<sup>-</sup>}. *Polyhedron*. 2008;27(6):1714-20.
  35. Momeni BZ, Rahimi F, Jebraeil SM, Janczak J. Supramolecular structures of Ni(II) and Pt(II) based on the substituted 2, 2': 6', 2"-terpyridine: Synthesis, structural characterization, luminescence and thermal properties. *Journal of Molecular Structure*. 2017;1150:196-205.
  36. Henderson MA. Photochemistry of methyl bromide on the α-Cr<sub>2</sub>O<sub>3</sub>(0001) surface. *Surface Science*. 2010;604(19-20):1800-7.
  37. Gilfrich J. Book review: Introduction to X-Ray Powder Diffractometry. RON JENKINS and ROBERT L. SNYDER Volume 138 in Chemical Analysis, J. D. Winefordner, Series Editor. Wiley, New York, 1996, pp. 403+xxiii, £65, ISBN 0471513393. *X-Ray Spectrometry*. 1997;26(4):245-